J Biomol NMR (2013) 55:47–58
DOI 10.1007/s10858-012-9685-7

ARTICLE

Measurement of rate constants for homodimer subunit exchange using double electron–electron resonance and paramagnetic relaxation enhancements

Yunhuang Yang · Theresa A. Ramelot · Shuisong Ni · Robert M. McCarrick · Michael A. Kennedy

Received: 14 August 2012 / Accepted: 4 November 2012 / Published online: 20 November 2012

Abstract Here, we report novel methods to measure rate constants for homodimer subunit exchange using double electron–electron resonance (DEER) electron paramagnetic resonance spectroscopy measurements and nuclear magnetic resonance spectroscopy based paramagnetic relaxation enhancement (PRE) measurements. The techniques were demonstrated using the homodimeric protein Dsy0195 from the strictly anaerobic bacterium *Desulfitobacterium hafniense* Y51. At specific times following mixing site-specific MTSL-labeled Dsy0195 with uniformly ^{15}N-labeled Dsy0195, the extent of exchange was determined either by monitoring the decrease of MTSL-labeled homodimer from the decay of the DEER modulation depth or by quantifying the increase of MTSL-labeled/^{15}N-labeled heterodimer using PREs. Repeated measurements at several time points following mixing enabled determination of the homodimer subunit dissociation rate constant, k_{-1}, which was 0.037 ± 0.005 min^{-1} derived from DEER experiments with a corresponding half-life time of 18.7 min. These numbers agreed with independent measurements obtained from PRE experiments. These methods can be broadly applied to protein–protein and protein-DNA complex studies.

Keywords DEER · PRE · EPR · NMR · Protein · Homodimer · Rate constants · Subunit exchange

Y. Yang · T. A. Ramelot · M. A. Kennedy (✉)
Department of Chemistry and Biochemistry, and Northeast Structural Genomics Consortium (NESG), Miami University, Oxford, OH 45056, USA
e-mail: kennedm4@muohio.edu

S. Ni · R. M. McCarrick
Department of Chemistry and Biochemistry, Miami University, Oxford, OH 45056, USA

Introduction

Proteins are commonly found to exist and function as homodimers, heterodimers, homo-oligomers, or hetero-oligomers (Mathhews and Sunde 2012). Indeed, a recent analysis of the Swiss-Prot database predicted that more than 86 % of proteins exist naturally as oligomeric complexes either as dimers (50 %) or higher-order oligomers (36 %) (Shen and Chou 2009). A similar analysis predicted >80 % of *Escherichia coli* proteins exist as homo-oligomers (Goodsell and Olsen 2000). Homo-oligomers have been found to represent the majority (50–70 %) of proteins with a known quaternary structure and the homo-oligomer assembly has been suggested to provide insight into the evolution of protein complexes (Levy et al. 2008). Furthermore, a genome-wide study of the yeast proteome indicated that the cellular proteins partitioned into 491 complexes that differentially combined to enable diversification of potential functions (Gavin et al. 2006) demonstrating the implicit importance of protein complex formation and dissociation.

Protein complexes can be grouped into distinct categories depending on the strength of the interaction between individual chains as defined by the equilibrium dissociation constant, K_d. At one extreme, protein complexes with subnanomolar K_ds are described as having "strong" interactions and are considered to exhibit "permanent" association. At the other end of the spectrum, protein complexes with greater than micromolar K_ds are described as having "weak" interactions and the corresponding complexes are considered "transient", existing in an equilibrium between monomer and oligomer forms that are freely able to exchange with each other (Vinogradova and Qin 2012). Interestingly, knowledge of the K_d for a given protein complex does not provide direct information regarding the

rate of subunit exchange, which, in the case of a predominantly oligomeric complex, is governed by the dissociation rate constant, k_{-1}.

The definition of K_d in terms of k_{-1} and k_1 implies that the half-life of different protein complexes with the same K_d can vary by several orders of magnitude, from minutes to years, depending on the values of k_{-1} and k_1. The kinetics of protein subunit exchange in homo- or hetero-multimeric protein assemblies, however, is largely unexplored, with the exception of αA-crystallin, for which subunit exchange has been investigated by both fluorescence resonance energy transfer (FRET) (Bova et al. 1997, 2000; Liang and Liu 2006) and mass spectrometry (Sobott et al. 2002; Aquilina et al. 2005). Notwithstanding, the kinetics and thermodynamics of subunit exchange in multimeric proteins is of great potential biological significance since proteins frequently have multiple functions in the cell that require exchanging binding partners in order to carry out specific biochemical or cellular functions.

The functional significance of transient protein–protein interactions in weak oligomeric complexes has been reviewed by Nooren and Thornton (2003). Several examples contained therein indicated that the transient nature of proteins in equilibrium can be directly related to their biological function. Despite the potential importance of weak transient interactions to the biological function of protein assemblies, experimental characterization of subunit exchange kinetics remains challenging and the literature addressing these issues is surprisingly sparse. A few studies investigating the biological significance of subunit exchange in oligomeric proteins include the histidine kinase EnvZ homodimer in Escherichia coli using cross-linking experiments (Cai and Inouye 2003), the HIV-1 protease dimer using fluorescence measurements (Darke et al. 1994) and Hepatitis B virus capsids using mass spectrometry (Uetrecht et al. 2010).

Besides its fundamental importance to biological function, there is a practical need to understand subunit exchange kinetics when preparing mixed labeled samples for solution-state NMR structure determination of homodimeric and oligomeric proteins. In particular, a ^{13}C-edited/^{12}C-filtered NOESY spectrum (Otting and Wüthrich 1989; Lee et al. 1994; Folmer et al. 1995) is routinely collected in order to determine NOEs that define the dimer interface using a mixed sample of a homodimeric protein in which one chain is uniformly ^{13}C-labeled and the carbon atoms of the other chain are at natural abundance, i.e. ^{12}C. Such a sample is prepared by mixing a pure sample of ^{13}C-labeled protein with a protein with the carbon atoms at natural abundance, and waiting for the subunit chains to exchange to produce a mixed ^{13}C-labeled/^{12}C-labeled sample. If subunit exchange occurs on the order of minutes, collection of the edited-filtered NOESY can proceed without delay, however, if the exchange occurs on the order of months or years, then collection of the dataset would be impractical.

Here, in order to broaden the array of experimental techniques available for investigation of subunit exchange kinetics in oligomeric proteins, we have developed novel pulsed electron paramagnetic resonance spectroscopy (EPR) double electron–electron resonance (DEER) and nuclear magnetic resonance spectroscopy (NMR) paramagnetic relaxation enhancement (PRE) based methods for measurement of rate constants for subunit exchange. While DEER and PREs have been widely applied to protein structure determination, protein–protein and protein-DNA complex structure determination (Battiste and Wagner 2000; Borbat et al. 2002; Hilger et al. 2007; Rumpel et al. 2008; Ward et al. 2009; Yang et al. 2010, 2011), transient intermediate detection (Iwahara and Clore 2006; Tang et al. 2006), characterization of dynamics of transient macromolecular interactions (Clore et al. 2007; Tang et al. 2007; Tang et al. 2008a, b) and weak protein–protein interactions (Jeschke et al. 2006a; Yu et al. 2009), these methods have not previously been used for measurement of homodimer protein subunit exchange rate constants. We demonstrated these new experimental approaches using the homodimer protein Dsy0195 from the strictly anaerobic bacterium *Desulfitobacterium hafniense* Y51.

Theoretical development

Our sample preparation strategy for measurement of rate constants for homodimer subunit exchange is summarized in Fig. 1. Two different protein forms were prepared: (*1*-oxy-2,2,5,5-tetramethyl-*D*-pyrroline-3-methyl)-methanethiosulfonate (MTSL)-labeled protein (referred to as M) and ^{15}N-labeled protein (referred to as N). Both protein forms were assumed to exist in equilibrium between monomer and dimer in solution as depicted in Fig. 1a and b, and represented by Eqs. (1) and (2), respectively. For a pure solution of M or N, the fraction of MM or NN dimer in solution will depend on the total protein concentration as governed by the dissociation constant K_d (Eqs. 1–2) where K_d is defined as k_{-1}/k_1 (or equivalently, k_{off}/k_{on}), and k_1 and k_{-1} (k_{on} and k_{off}) refer to the association and dissociation rate constants, respectively. The homodimer dominates the equilibrium when K_d is small relative to the total protein concentration. For example, the dimer fraction would be greater than 90.0 % when K_d is 100 times smaller than the total protein concentration. Knowledge of K_d, however, does not provide direct information about the kinetics of subunit exchange. In our case, since we are concerned with proteins that exist predominantly as homodimers or homo-oligomers in solution, our goal was

to design experiments that enabled direct measurement of k_{-1}, which would be rate limiting for subunit exchange.

In order to further develop our theory, any small potential structural differences that might affect the kinetics of subunit exchange caused by MTSL- or ^{15}N -labeling were neglected and K_d, k_1 and k_{-1} were assumed to be the same for MTSL-labeled, ^{15}N-labeled, and native unlabeled proteins. The assumption that MTSL-labeling does not alter the kinetics of homodimer dissociation can be cross-validated, even in the absence of knowledge of the structure, using the methods described below by repeating the k_{-1} measurements with MTSL labeling in multiple positions in the amino acid sequence.

Based on these assumptions, and assuming that K_d was small compared to the total protein concentration, the dimer species will be dominant in solution after mixing solutions of M and N and the subunits will exchange at a rate limited by k_{-1}. Initially, at time t = 0, no MTSL-/^{15}N-labeled heterodimer (MN) will be present in solution. Over time, however, MN will form in solution from association of free M and N monomers as indicated in Eq. (3) resulting in time-dependent concentrations of MM, NN, and MN (Fig. 1c) until equilibrium is reached.

$$\mathrm{MM} \underset{k_1}{\overset{k_{-1}}{\rightleftarrows}} \mathrm{M} + \mathrm{M} \tag{1}$$

$$\mathrm{NN} \underset{k_1}{\overset{k_{-1}}{\rightleftarrows}} \mathrm{N} + \mathrm{N} \tag{2}$$

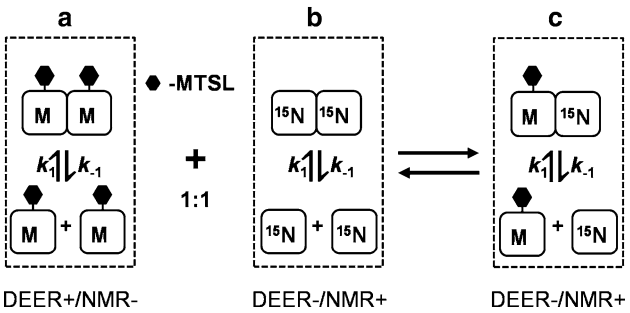

Fig. 1 General strategy for measurement of rate constants for homodimer subunit exchange. **a** represents the equilibrium between MTSL-labeled protein homodimer (MM) and MTSL-labeled monomer (M). **b** represents the equilibrium between ^{15}N-labeled protein homodimer (NN) and ^{15}N-labeled protein monomer (N). **c** represents the equilibrium between the MTSL-/^{15}N-labeled protein heterodimer (MN) and the individual monomer species (M) + (N). The 1:1 ratio indicates that equal concentrations of **a** and **b** are mixed in equal volumes. After mixing, the MN heterodimer depicted in (c) will be produced as the subunits undergo exchange. Under these conditions, three distinct dimer species, MM, MN, and NN, will exist in a 1:2:1 ratio at equilibrium. The k_1 and k_{-1} refer to the association and dissociation rate constants for each dimer/monomer equilibrium, respectively. DEER+/NMR+ means detectable by DEER/NMR, and DEER-/NMR- means not detectable by either technique

$$2 \times \left\{ \mathrm{M} + \mathrm{N} \underset{k_{-1}}{\overset{k_1}{\rightleftarrows}} \mathrm{MN} \right\} \tag{3}$$

In the special case where M and N are mixed at a 1:1 ratio, the premixing concentration of MM or NN will be equal to the total dimer concentration after mixing. Even though the overall dimer concentration in solution remains constant after mixing, it will become redistributed among three species, MM, NN and the MN. The net redistribution exchange process can be described by Eq. (4):

$$\mathrm{MM} + \mathrm{NN} \underset{k_{-1}}{\overset{k_{-1}}{\rightleftarrows}} 2\mathrm{MN} \tag{4}$$

Since k_{-1} is rate-limiting for subunit exchange, this dissociation rate constant will also govern the rate at which equilibrium is established between dimer forms as indicated in Eq. (4). Under the special case described above, a statistically predictable 1:2:1 distribution of dimer species MM, MN and NN will be present in solution at equilibrium.

Equation (4) is potentially confusing since it represents the sum of Eq. (1) through (3) and indicates that the overall equilibrium constant K_{eq} for subunit exchange is equal to 1. Eq. (4) indicates that the rate constant governing subunit exchange in either direction is k_{-1} (k_{off}). This is true because in order to reach the overall equilibrium, MM must dissociate into M + M, NN must dissociate into N + N, and MN must dissociate into M + N. Thus, both the forward and backward rates in eq. (4) are limited by k_{-1}. Therefore, K_{eq}, defined as the ratio of the rate constants for the forward to backward reactions, is equal to k_{-1}/k_{-1}, i.e. $K_{eq} = 1$. This conclusion is confirmed by applying the rules governing calculation of the equilibrium constant for simultaneous equilibria (where the overall equilibrium constant is the product of the equilibrium constants for each reaction), which yields an overall $K_{eq} = 1$.

General considerations for experimental measurement of k_{-1} using DEER or PREs

The DEER EPR experiment can detect the presence of MTSL-labeled dimers in solution due to the intra-dimer dipolar interaction between unpaired electrons in the nitroxide radical of the MTSL group covalently attached to each subunit. Specifically, the DEER modulation depth reports on the concentration of MM in solution. Among the three dimer species that can form after mixing solutions of M and N, only MM can contribute to the DEER modulation depth while MN can only contribute to the DEER background due to inter-dimer dipolar interactions between unpaired electrons, and NN is not detectable by DEER or EPR and can not contribute to the DEER modulation depth.

The NMR PRE experiments can detect the presence of MTSL-labeled protein/^{15}N-labeled protein heterodimers (MN) from changes in amide proton to amide nitrogen cross peak intensities measured from two-dimensional ^{1}H-^{15}N heteronuclear single quantum coherence (HSQC) or heteronuclear multiple quantum coherence (HMQC) experiments. PREs can only be detected in MN species while NN homodimers produce NMR spectra free from PREs and no NMR signal can be detected from MM homodimers.

A fundamental requirement for experimental determination of rates of homodimer or heterodimer subunit exchange is the ability to measure the amount of MM or MN in solution as a function of time. The DEER and PRE based experiments described above enable such measurements. A further requirement is determination of the order of the kinetics of subunit exchange, which was determined to be first-order.

According to first order kinetics, the concentration of the MM dimer will decrease over time according to a single exponential decay as a function of the product of the dissociation rate constant k_{-1} and the exchange time, t. Therefore, a plot of the decay of the DEER modulation depth or NMR cross peak intensity as a function of the exchange time as the system moves from its initial state towards equilibrium can be fit to a single exponential decay to determine k_{-1}. The explicit mathematical expressions derived for both DEER EPR and PRE NMR experiments are developed below.

DEER modulation depth analysis and simulations

Over the course of subunit exchange, the DEER modulation depth depends on the amount of MM in solution. The DEER modulation frequency depends on the dipole–dipole interaction between unpaired electron spins, i.e. the distribution of distances between the two MTSL nitroxides. For a solution of specific site-directed MTSL-labeled dimer, the distance distribution between the two nitroxides will be constant when the protein exists as a homodimer and DEER modulation frequency will be constant. The only factor that can alter the DEER modulation depth over the course of subunit exchange is a change in the concentration of MM. When M and N are mixed in a 1:1 ratio, DEER modulation depth will decay according to Eq. (5):

$$\frac{I(t)}{I_0} = 0.5 \times \exp(-k_{-1}t) + 0.5 \quad (5)$$

Here, I(t) stands for the DEER modulation depth at a given subunit exchange time t, and I_0 indicates the initial DEER modulation depth at $t = 0$ prior to subunit exchange. Note that in the limit of $t >> 1/k_{-1}$, which would be the case at equilibrium, I(t) decays to 50 % of I_0. The simulation decay curve for this process is depicted in Fig. 2 for the 0.5 ratio of [MM] to the sum of homodimers ([MM] + [NN]).

Homodimer dissociation rate constants can be determined for homodimer K_d values up to ~1–5 mM using this EPR DEER method for 1:1 mixtures of MM and NN. The upper limit in K_d is related to the maximum protein concentration that can be used for DEER experiments in order to avoid significant intermolecular dipolar background signals that would interfere with data analysis, which is about 500 μM, but can be higher depending on the specific protein under investigation. If we assume that the DEER experiment can work over a range of 10–500 μM MM concentration, then, for a total starting protein concentration of 500–100 μM with a dimer dissociation constant $K_d = 1$ mM, the MM concentration at equilibrium will range from 134 to 8.5 μM. After mixing with an equal amount of NN dimer, the labeled dimer concentration at equilibrium will fall in the range of 67–4.3 μM, well within the measurable range of the DEER experiment. For a total starting protein concentration range from 500 to 100 μM with a dimer dissociation constant $K_d = 5$ mM, the initial MM concentration would range from 42 to 2 μM. After mixing with an equal amount of NN, the MM concentration at equilibrium will fall in the range of 21–1 μM, where the upper limit falls in the measurable range of the DEER experiment. Clearly at the upper limit $K_d = 5$ mM, one would have to work at the highest possible total protein concentration in the available range. When higher protein concentrations near ~500 μM or above are used for DEER measurements, the intermolecular background signal can become large relative to the modulation depth itself

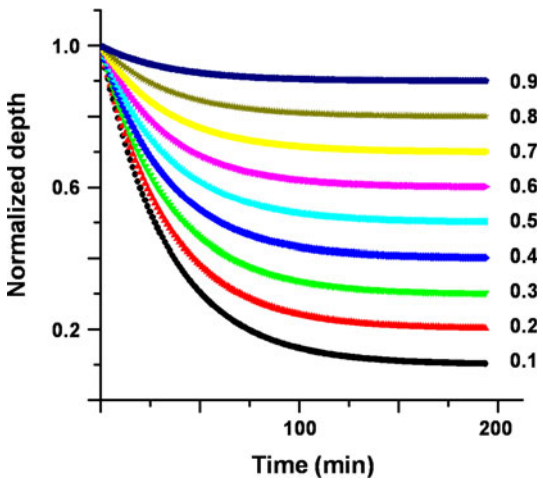

Fig. 2 Simulation of DEER modulation depth versus subunit exchange time according to Eq. (6). The initial fraction of MM out of the total dimer concentration, $[MM]_0/([MM]_0 + [NN]_0)$, is indicated at the right of each curve. A $k_{-1} = 0.037$ min^{-1} was used in Eq (6) for the simulations

and must be subtracted prior to analysis of the DEER modulation depth introducing an increasing risk of error in the determination of the DEER modulation depth, especially in a series of time measurements.

In general, it is not necessary to mix equal amounts of M and N in order to measure k_{-1}. The initial concentration of MM in solution and the final ratio of MM:MN:NN dimers will depend on the ratio of concentrations of M to N in solution, as depicted in Fig. 2. The general expression for the DEER modulation depth as a function of time is given by Eq. (6):

$$\frac{I(t)}{I_0} = \frac{[NN]_0}{([MM]_0 + [NN]_0)} \times \exp(-k_{-1}t) + \frac{[MM]_0}{([MM]_0 + [NN]_0)} \quad (6)$$

Here, $[MM]_0$ and $[NN]_0$ stand for the initial dimer concentrations before subunit exchange, the $[NN]_0/([MM]_0 + [NN]_0)$ term represents the fraction of MM exchanged at equilibrium, and $[MM]_0/([MM]_0 + [NN]_0)$ represents the non-exchanged fraction of MM. A decreasing fraction of MM in the mixture would be associated with a larger decay in the DEER modulation depth (Fig. 2). These simulated DEER decays can be used to optimize experiments to achieve the best fit of DEER modulation depth decay.

PRE analysis and simulations

The dissociation rate constant k_{-1} can also be determined from a time-course analysis of PREs. However, the data analysis is complicated by the fact that at any given time during exchange, the NMR cross peak intensity for any amide proton in the ^{15}N-labeled chain is a sum of intensity contributions from NN, N, and MN, where the intensity contribution from MN depends on the magnitude of the PRE for a given residue. For the special case of a 1:1 mixture of M and N in a 1:1 volume ratio, the observed NMR signal can be described by the Eq. (7):

$$\frac{I(t)}{I_0} = \{0.5 \times \exp(-k_{-1}t) + 0.5\} + \frac{I_{para}}{I_{dia}}\{0.5 \times [1 - \exp(-k_{-1}t)]\} + \frac{I_N}{I_0} \quad (7)$$

Here, I(t) stands for the observed NMR cross peak intensity at a given subunit exchange time t, I_0 stands for the observed NMR cross peak intensity before subunit exchange, and I_N stands for NMR cross peak intensity from the N monomer in solution. I_{para} stands for the NMR cross peak intensity from a given amide proton in the MN heterodimer, and I_{dia} stands for the NMR cross peak intensity from a given amide proton in the absence of PREs. The PRE magnitude from MN for any given amide is dependent on its distance distribution to the nitroxide of MTSL, which should be constant for all MN heterodimers. I_{dia} can be easily estimated from NN.

Similar to the DEER method, k_{-1} can be determined using the NMR PRE method for the homodimers with K_d up to $\sim$1 mM, beyond which the small dimer concentration in solution would limit the PRE measurements. For example, if a 1 mM protein solution was prepared for a protein with a $K_d \sim 1$ mM, only $\sim$40 % of the protein would remain in solution in the dimer form at equilibrium, i.e. the total dimer concentration would be $\sim$0.4 mM, and furthermore, the dimer species would be distributed over MM, MN and NN, so the concentration of MN would be just 0.2 mM and the concentration of NN would be 0.1 mM. Therefore, measurement of PREs and decay curves at these concentrations would be at the practical limit of detection for the NMR technique.

In general, when unequal amounts of M and N are mixed, the observed NMR cross peak intensity in PRE experiment can be described by Eq. (8):

$$\frac{I(t)}{I_0} = \left\{\frac{[MM]_0}{([MM]_0 + [NN]_0)} \times \exp(-k_{-1}t) + \frac{[NN]_0}{([MM]_0 + [NN]_0)}\right\} + \frac{I_{para}}{I_{dia}}\left\{\frac{[MM]_0}{([MM]_0 + [NN]_0)} \times [1 - \exp(-k_{-1}t)]\right\} + \frac{I_N}{I_0} \quad (8)$$

Here, $[MM]_0$ and $[NN]_0$ stand for the initial dimer concentrations before subunit exchange. The NMR signal contribution from monomer N can be neglected when [N] is small relative to either [NN] or [MN] in the final equilibrium, which will be true when K_d is much smaller than the total protein concentration.

The time-dependent NMR signal following mixing equal amounts of M and N during subunit exchange was simulated following using Eq. (8), where I_{dia} was normalized and k_{-1} of 0.037 min^{-1} was used (Fig. 3a, b). Figure 3a shows the simulated exponential decay of the ^{1}H-^{15}N HSQC or HMQC cross peak intensity of NN, and exponential growth of the ^{1}H-^{15}N HSQC or HMQC cross peak intensity of MN for three different PREs magnitudes indicated by I_{para}: strong PRE ($I_{para} = 0$), medium PRE ($I_{para} = 0.5$) and weak PRE ($I_{para} = 1$). Figure 3b illustrates the simulated time-dependent NMR signal intensity, which is the sum of NN and MN contributions, for the three different PRE magnitudes over the course of subunit exchange. If weak or no PREs can be observed, as is the case for amide proton to nitroxide distances greater than $\sim$30 Å (Battiste and Wagner 2000), the overall NMR signal will not change upon mixing and it would not be possible to derive k_{-1} from cross peaks for these residues. On the other hand, when PREs can be measured, it is possible to derive k_{-1} from fitting the decay of the ^{1}H-^{15}N HSQC or HMQC cross peak intensity as a function of time.

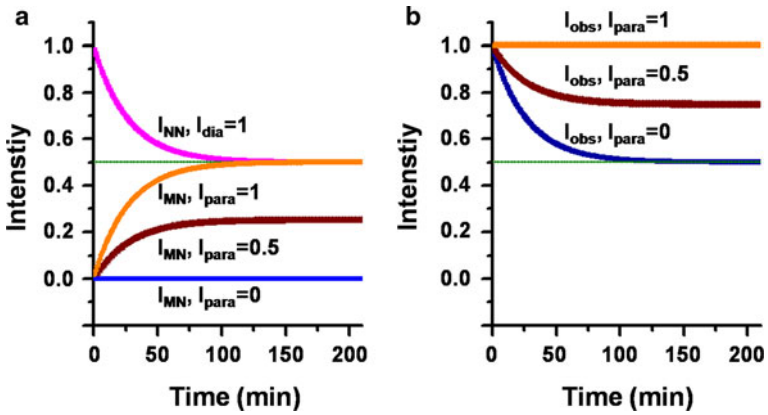

Fig. 3 Simulation of NMR cross peak intensity versus subunit exchange time for the PRE experiment using Eq (8). **a** Simulation of NMR cross peak intensity decay from NN (I_{dia}, normalized to 1, magenta) versus mixing time, and growth from MN for three different PRE magnitudes indicated by I_{para}, which was normalized to I_{dia} (orange, $I_{para} = 1$; wine, $I_{para} = 0.5$; and royal, $I_{para} = 0$). The olive line stands for the intensity of 0.5. **b** The summation of the NMR signal intensity (I_{obs}) from NN and MN. k_{-1} of 0.037 min^{-1} was used in Eq. (8) for the simulations

For a dimer with K_d much smaller than the total protein concentration required for PRE experiment ($\sim$0.3–1.0 mM typically), the magnitude of the overall NMR signal decay is not only dependent on the magnitude of PRE, but also on the initial M and N concentration ratio. Figure 4 shows the simulated NMR signal decay for a series of NN fractions of the total dimer concentration as indicated (Fig. 4d), also for different PRE magnitudes. From Fig. 4, it is evident that smaller fractions of NN and stronger PREs lead to greater magnitudes of ^{1}H-^{15}N HSQC or HMQC cross peak decay.

Materials and methods

Preparation of protein samples

Samples for DEER and PRE measurements were prepared as previously described for determination of the solution NMR structure of Dsy0195 (Yang et al. 2010, 2011) including the protein construct, expression and purification, characterizations of dimeric state in solution, and site-directed spin labeling of Dsy0195-S36C-MTSL/Dsy0195-S52C-MTSL.

DEER experiments

^{15}N- and MTSL-labeled Dsy0195-S36C samples were dissolved in buffer containing 20 mM NH_4OAc, 200 mM NaCl, and 5 mM $CaCl_2$ (pH 4.5) diluted to a final concentration of 30 % (w/w) glycerol. The final sample concentration was about 0.2 mM. The exchange rate was assumed to be independent of the presence of 30 % glycerol and flash freezing, which was confirmed by comparison with the exchange measurements using the NMR-based PRE method in the presence of the presence of 10 % glycerol. All DEER experiments were carried out at Q-band (34 GHz) on a Bruker ELEXSYS E580 pulsed EPR instrument at 80 K. Each DEER experiment required 12.5 min of data acquisition.

DEER experiments were repeated five times on a control sample (0.1 mM, diluted by buffer). The mixtures of ^{15}N-/MTSL- labeled Dsy0195-S36C (each 0.1 mM) were prepared at ten mixing times: 2.5, 5, 10, 15, 25, 35, 52.5, 70, 112.5, 155 min. Each sample ($\sim$20 μL) was put into an EPR capillary tube at the selected mixing time at room temperature (293 K), and then flash frozen in liquid nitrogen immediately before DEER data collection. Each DEER time point measurement was repeated.

All DEER spectra were analyzed using Tikhonov regularization simulations with DeerAnalysis2011 (Jeschke et al. 2006b) to eliminate three-dimensional homogeneous background contributions from intermolecular interactions. The resulting spectra were scaled so that the maximum had a value of 1. The modulation depth for each spectrum was measured by taking 1—the spectrum minimum. For the series of exchange experiments shown in Fig. 5, the modulation depth of the initial t = 0 spectrum was scaled to 1 and the modulation depths calculated for the remaining exchange spectra were scaled with the same factor.

PRE experiments

^{15}N- and MTSL-labeled Dsy0195-S52C samples were dissolved in buffer containing 20 mM NH_4OAc, 200 mM NaCl, 5 mM $CaCl_2$ (pH 4.5), 10 % D_2O, and 10 % (w/w) glycerol. The final sample concentration was about 0.6 mM. One control sample ^{15}N-Dsy0195-S52C (0.3 mM, diluted by buffer) was prepared in order to estimate the inherent cross peak intensity error. This control experiment was repeated 10 times at 10 min intervals. The ^{15}N-/

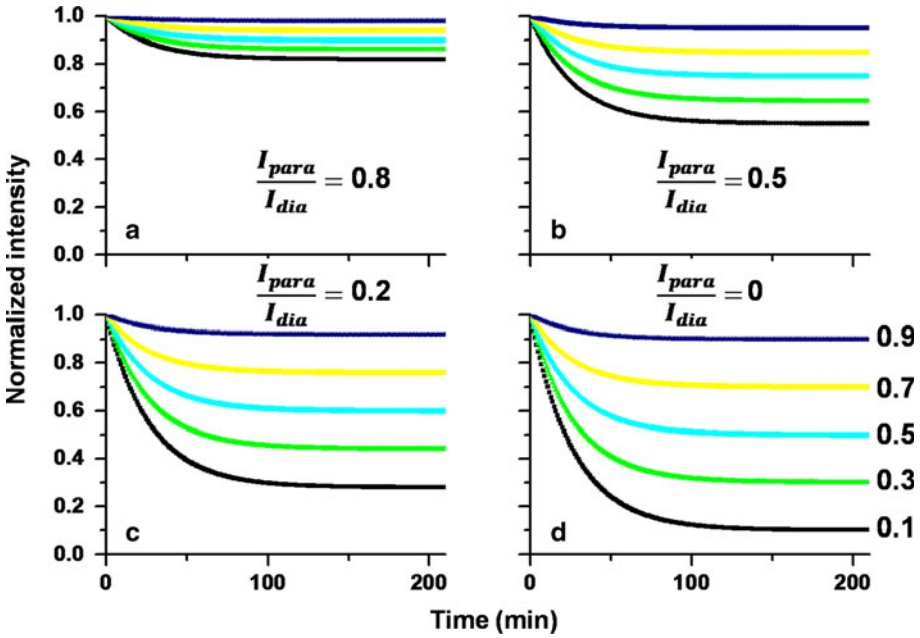

Fig. 4 Simulation of NMR cross peak intensity versus subunit exchange time for PRE experiments for a series of NN concentration fractions of the total dimers $[NN]_0/([MM]_0 + [NN]_0)$ as indicated. **a** Simulation curves with PREs indicated by I_{para}/I_{dia} of 0.8. **b** I_{para}/I_{dia} of 0.5. **c** I_{para}/I_{dia} of 0.2. **d** I_{para}/I_{dia} of 0. k_{-1} of 0.037 min^{-1} was used with Eq. (8) for simulations

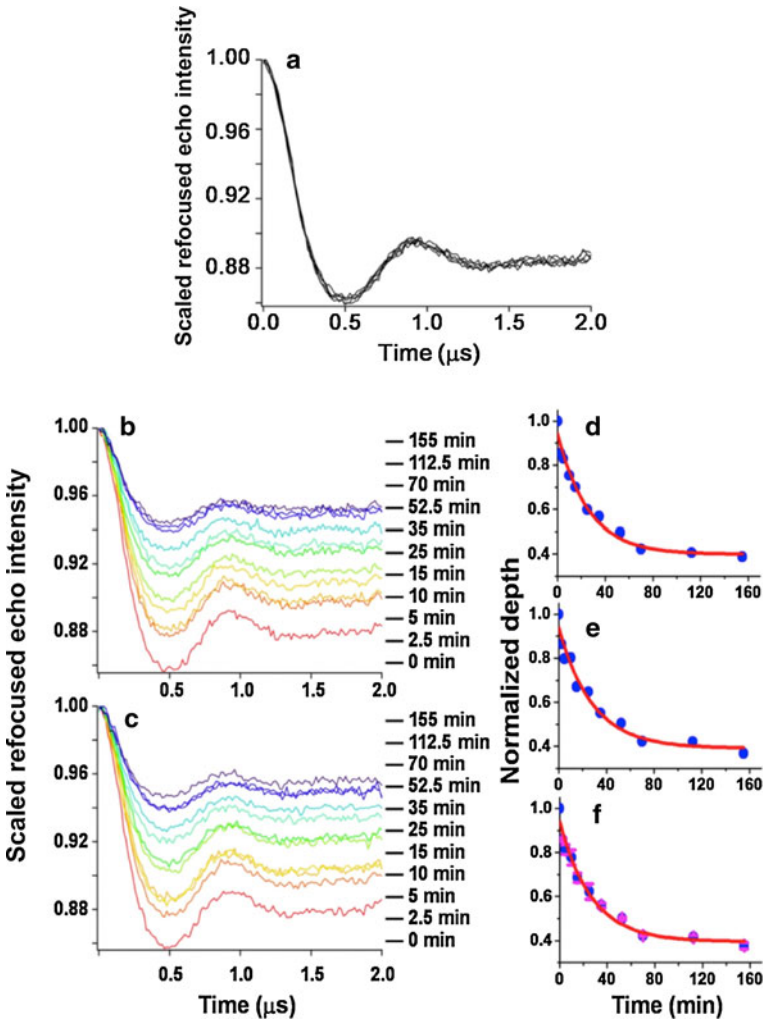

Fig. 5 Time-domain DEER signals and fits of modulation depth decay curve versus mixing time to determine k_{-1} values. **a** Overlay of the scaled refocused echo intensity for five repeated DEER experiments of 0.1 mM Dsy0195-S36C-MTSL. **b** Time-domain DEER signals of 1:1 mixtures of Dsy0195-S36C-MTSL/^{15}N-Dsy0195-S36C at a series of exchange time points indicated in order, from bottom to top, at right. Exchange took place at room temperature (293 K). The repeated DEER experiments are shown in **c**. Fits of the experimental data to a single exponential decay for data in **b** and **c** are shown in **d** and **e**, and the best fit of the exponential decay to the average of the modulation depth versus exchange time is shown with error bars in **f**

MTSL- labeled Dsy0195-S52C (total 300 µL) were mixed at 1:1 ratio at 298 K before PRE data collection. The PRE experiment was repeated at the following exchange times: 6, 8, 10, 15, 20, 25, 35, 45, 52.5, 60, 70, 90, 112.5, 140, 155, 180 and 210 min.

All PRE experiments were performed using the 2D SOFAST-HMQC pulse sequence (Schanda and Brutscher 2005). The NMR data collection parameters were as follows: recycling time $t_{rec} = 100$ ms, 40 complex points in the second dimension (^{15}N) with sweep width of 29 ppm, $t_1^{max} = 23$ ms, $t_2^{max} = 47$ ms, the total experiment time for each spectrum is 58 s. The flip angle for the first proton pulse was 120°. The band-selective ^{1}H pulses were centered at 8.0 ppm covering a bandwidth of 4.0 ppm. All NMR spectra were collected on a Bruker Avance 600 MHz NMR spectrometer at 293 K, processed using NMRPipe, and analyzed by SPARKY.

Results and discussion

Experimental EPR-based DEER measurements of subunit exchange

The Dsy0195-S36C mutant was prepared for DEER experiments since the distance between S36 C_β atoms in the two subunits of the homodimer (~32 Å) (Yang et al. 2010) was suitable for DEER measurements (~15–80 Å) (Pannier et al. 2000). Initial attempts at collection of a time series of DEER measurements using a single sample proved unsuccessful due to freeze–thaw cycling introducing uncertainty into the exchange time period. Alternatively, a series of identical samples were prepared and allowed to undergo exchange for different periods of time prior to flash freezing and DEER data collection. In order for this approach to work, it was necessary to demonstrate high reproducibility of measurement of the DEER modulation depth for repeated insertions of EPR sample tubes into the resonant cavity. After carefully controlling the insertion depth for repeated sample insertions, we were able to achieve highly reproducible data for repeated measurements. To illustrate the reproducibility of repeated measurements, five repetitions of the DEER experiment were collected on a control sample of Dsy0195-S36C-MTSL (Fig. 5a). The results indicated that quantitative measurement of the DEER modulation depth was highly reproducible. The exchange time for the series of DEER experiments could be precisely and accurately controlled since each mixed sample was flash frozen in liquid nitrogen immediately before data collection.

Figure 5b shows the intensity of the DEER modulation depth for a series of exchange times corresponding to 0, 2.5, 5, 10, 15, 25, 35, 52.5, 70, 112.5 and 155 min after mixing MTSL-labeled Dsy0195 and ^{15}N-labeled Dsy0195. The DEER modulation depth decreased with increasing exchange time (Fig. 5d), as expected, indicating a decreasing fraction of MM homodimer in solution over time. The DEER time course experiment was repeated and found to be highly reproducible (Fig. 5c, 5e). The mean modulation depth versus exchange time fit well to a first order exponential decay as shown in Fig. 5f. The k_{-1} derived from the fitted curve was 0.037 ± 0.005 min^{-1} indicating a homodimer half-life time of about 18.6 min.

While it was not possible to experimentally determine the homodimer dissociation constant K_d from the data collected here, one could estimate the lower limit for K_d using the diffusion-limited value of k_1 (Smoluchowski 1917; Gabdoulline and Wade 2002) and then apply the definition of $K_d = k_{-1}/k_1$, i.e. k_{off}/k_{on} however, this would likely result in a highly inaccurate estimate of K_d. Alternatively, one could use more sophisticated approaches to compute k_{on}, such as Brownian dynamics (Gabdoulline and Wade 2002; Scholosshauer and Baker 2004) presumably leading to a more accurate estimate of K_d.

Experimental NMR-based PRE measurements of subunit exchange

NMR PRE experiments were conducted in solution after a specified mixing time. In contrast to EPR DEER experiments, subunit exchange continued during NMR PRE data collection. This is a potential problem if the exchange rate is comparable, or fast, relative to the time required for data collection. To minimize this problem, rapid data collection was accomplished using a 2D band-selective optimized flip-angle short-transient ^{1}H-^{15}N heteronuclear multiple quantum coherence (SOFAST-HMQC) (Schanda and Brutscher 2005) experiment for PRE measurements. Spectra obtained in this fashion required only 58 s total acquisition time for each exchange time point measurement and the exchange time was considered to be at the midpoint of the data collection time. The mutant Dsy0195-S52C was prepared for NMR PRE experiments since the distance between the S52 C_β atoms in the two subunits of the homodimer (~15 Å) was expected to produce measurable PREs (<22 Å) (Yang et al. 2010).

Since the rate constant for subunit exchange would be derived from a fit of the decay of ^{1}H-^{15}N HMQC cross peaks as a function of exchange time, we first set out to determine the magnitude of the intrinsic experimental variation in cross peak intensities due to repeated measurements on the same sample. In order to estimate the inherent cross-peak intensity error for a series of time-course measurements, ten repetitions of 2D SOFAST-

HMQC spectra were collected on a control sample of 0.3 mM ^{15}N-Dsy0195-S52C. From these data, we evaluated the normalized amide proton to amide nitrogen cross-peak intensity for ~39 amino acids and found that the intensity fluctuated by up to 15 % about the normalized mean (Fig. 6a), which indicated that averaging of multiple NMR PRE measurements would be required for a reliable fit and accurate determination of k_{-1}.

A series of 2D SOFAST-HMQC spectra of the mixed sample of MTSL-labeled Dsy0195 and ^{15}N-labeled Dsy0195 were collected at exchange times 6, 8, 10, 15, 20, 25, 35, 45, 52.5, 60, 70, 90, 112.5, 140, 155, 180 and 210 min. As subunit exchange proceeded, an increasing amount of MN dimer was evident as indicated by weaker, broader peaks for some residues, including L79, Y81 and E84 (Fig. 6b–e). The maximum PRE would lead to a 50 % decrease in cross peak intensity for 1:1 mixing of the homodimer mixture as indicated previously (Rumpel et al. 2008). No chemical shift effects/differences were observed between the monomer and dimer species undergoing exchange. The PRE experiment was repeated four times at each time point using different samples for signal averaging. After NMR data collection and processing, 39 non-overlapped cross peaks were chosen for analysis. The k_{-1} was derived by fitting the decay of the NMR cross peak intensity as a function of exchange time. Although the PREs could be quantified in terms of distances, this was not necessary to determine k_{-1}.

The resulting first-order exponential decay curve fits are shown for the averaged normalized cross peak intensities versus exchange time for residues L79, Y81 and E84 (Fig. 6f-h). The corresponding k_{-1} values derived from the decay curves were 0.033 ± 0.013, 0.040 ± 0.011 and 0.037 ± 0.008 min^{-1}, respectively. Although the mean value of k_{-1} (0.037 min^{-1}) was consistent with that determined from the DEER experiments, the uncertainty in k_{-1} derived from the PRE measurements was larger as indicated by the error bars in the fitted curves. Weaker PREs were detected for other peaks from residues located farther from the MTSL on the other subunit, however, only peaks for residues L79, Y81 and E84, which were located on the interface relatively close to the interchain MTSL nitroxide and had strong PREs, were fit to acceptable accuracy.

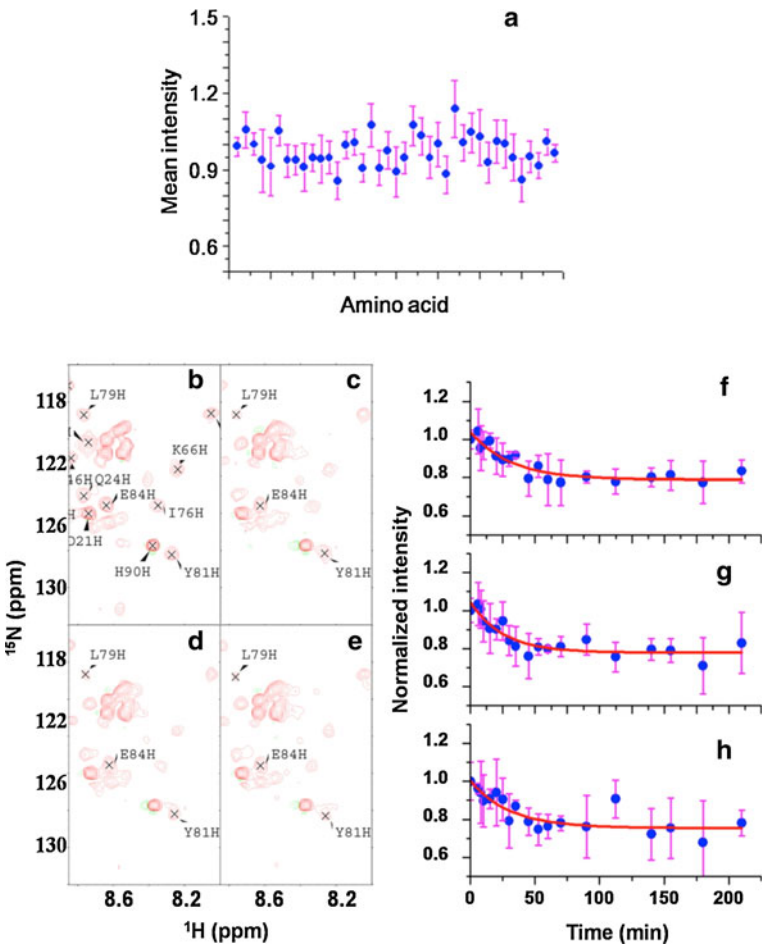

Fig. 6 PRE experiments and fitted curves for determination of k_{-1} values. (a) Average normalized intensity of 39 non-overlapped peaks from ten-repeated 2D SOFAST-HMQC data sets collected on 0.3 mM Dsy0195-S52C. 2D SOFAST-HMQC spectra of 0.3 mM ^{15}N-Dsy0195-S52C (**b**), and of a 1:1 mixture of ^{15}N-Dsy0195-S52C/Dsy0195-S52C-MTSL (each 0.3 mM) at exchange times of 6 (**c**), 70 (**d**), and 180 min (**e**), respectively. Three cross peaks corresponding to residues L79, Y81 and E84 are labeled, for which peak broadening from PREs is clearly evident. The final averaged, normalized cross peak intensities, and associated errors, versus exchange time from amino acids L79, Y81 and E84 were fitted and shown in (**f**), (**g**), and (**h**)

Advantages and disadvantages of DEER and PRE based measurements of subunit exchange

We have demonstrated that rate constants for homodimer subunit exchange can be determined using either NMR-based PRE measurements or EPR-based DEER measurements. The two techniques are complementary in that they enable independent measurement of the dissociation rate constant, k_{-1}, and that they are applicable over different distance ranges between the MTSL spin labels and/or ^{15}N-labeled amino acids. Since only MTSL-spin labeling of the protein, in addition to preparation of unlabeled protein for mixing, is required for the EPR-based DEER technique, it can be potentially applied to a wide array of samples including protein–protein and protein-DNA complex exchange studies. Furthermore, since the DEER effect is measureable for MTSL labels separated by up to ~80 Å (Pannier et al. 2000), the EPR-based DEER technique has effectively no upper molecular weight limit, as long as the protein complex is soluble in the range of 10–500 μM in solution. The NMR PRE-based technique has the additional requirement that ^{15}N-labeled protein must be prepared for mixing, and that it must be possible to collect a ^{1}H-^{15}N HSQC or HMQC that has at least some resolved cross peaks with measureable PREs. This latter requirement restricts the method to the normal molecular weight upper limit as for protein structure determination using traditional solution state NMR methods, i.e. ~25 kDa in non-deuterated proteins, or >25 kDa in deuterated proteins and using TROSY methods (Pervushin et al. 1997).

The DEER and PRE methods have their own specific advantages and disadvantages. One requirement, and limitation, common to both is that the protein must be spin-labeled. The standard way to accomplish this is to introduce a site-specific spin label by covalently modifying a single cysteine in the protein with MTSL. Generation of a protein containing a single cysteine, however, may often require site-directed mutagenesis. In the application of DEER and PREs introduced here, however, since we need not extract distance information, it is not necessary to produce a protein containing a single cysteine. Rather, the technique should work equally well if multiple cysteines are present and modified in a single protein, as long as the T_2 of the unpaired electron is suitable, i.e. not too short, for DEER measurements. The electron T_2 is determined by the local spin density around the unpaired electron, which is dominated by the dipolar interaction with the unpaired electron in the nitroxide radical on the MTSL group of the other homodimer subunit. Since the sample is frozen during the DEER measurement, the electron T_2 will be independent of either the dissociation rate constant k_{-1} or the equilibrium dissociation constant K_d since the spin density around the nitroxide radical is constant over the course of the DEER measurement. Even if the measurement were made in solution, the electron T_2 values would be unaffected by the rate of dimer dissociation since the electron T_2 values are on the order of microseconds, while the dissociation rate constants amenable to DEER measurement are on the order of minutes or longer. Therefore, the dimer would appear static on the timescale of electron relaxation.

Multiple MTSL labels on a single protein chain may produce a DEER signal that is difficult or impossible to interpret, however, it would lead to a near ideal response for PRE measurements, with more residues on the ^{15}N-labeled chain experiencing strong PREs, producing the largest possible change in cross peak intensity upon mixing, and therefore greatest sensitivity for determination of k_{-1}. One caveat in having multiple MTSL labels on a single protein chain is that the binding affinity may be significantly affected. Alternatively, the protein sequence can be modified to introduce a specific metal binding site, such as an lanthanide binding tag (LBT) (Cooper et al. 2008; Yagi et al. 2011), to engineer any protein to bind single paramagnetic Gd^{3+} ion, which could then be used for DEER and PRE measurements in a protein with any number of naturally occurring cysteine residues.

After one or more paramagnetic spins have been introduced into the protein, the DEER method requires a much lower protein concentration (~0.01–0.5 mM) for data measurement compared to that required for NMR measurements (~0.3–1 mM) due to the greater intrinsic sensitivity of EPR compared to NMR. The study reported here benefited greatly by the sensitivity gained from Q-band DEER experiments (Ghimire et al. 2009; Polyhach et al. 2012), which if not available, would greatly decrease the sensitivity advantage enjoyed by the EPR technique. The lower sample concentration actually benefits the DEER experiment as long as sufficient signal intensity is available to measure the DEER modulation depth.

This is due to reduction in background contributions from interdimer dipolar interactions that can be significant at protein concentrations greater than about 0.1 mM, which require increasing dependence on background subtraction to be able to interpret the data.

The DEER experiment also requires substantially less sample volume (~10–20 μL) compared to the NMR experiments (~250 μL), resulting in a substantially smaller overall sample requirement. Furthermore, the DEER approach requires only MTSL or LBT-based spin-labeling, whereas, either MTSL or LBT spin-labeling and ^{15}N-labeling is required for NMR-based PRE measurements. However, when both EPR and NMR techniques can be used, the ^{15}N-labeled sample can be used for both DEER and PRE experiments. Application of both

techniques offers the advantage of independent determination and validation of k_{-1}. Finally, DEER modulation can be detected over a much greater range of distances between spin labels ($\sim$15–80 Å) compared to the relatively narrow range of distances (<30 Å) suitable for PRE measurements.

One obvious advantage of the NMR PRE method is that it can be conducted if pulsed EPR at Q-band is unavailable. Another advantage of the PRE approach is that independent determinations of k_{-1} can be made using multiple amino acid residues from a single spin-labeled protein sample, in contrast, to the DEER methods, which allows only a single measurement of k_{-1} from a single spin-labeled sample. A disadvantage of the PRE approach is that several replicated data sets must be collected to produce acceptable accuracy due to the intrinsic random fluctuations of the cross peak intensities, compared to the highly reproducible DEER decay profiles observed in this study.

Finally, considering the experimental data collection time required for both methods, the DEER method can monitor relatively fast exchange processes compared to the NMR PRE method, with the DEER method being limited only by the time it takes to freeze the sample after mixing, since the exchange process is quenched upon freezing. Assuming the first DEER point is collected at a minimum exchange time of 1 min, and assuming $t_{1/2}$ is approximately 5 min, the largest dissociation rate constant that can be measured using DEER is $(\ln 2)/5 = 0.14\ \text{min}^{-1}$. For subunit exchange $t_{1/2}$ longer than 5 min, both the DEER and PRE methods are practical and reliable.

Conclusions

In conclusion, the PRE- and DEER-based approaches introduced here for measurement of rate constants for subunit exchange in protein complexes should be of broad general interest. While FRET and nanoelectrospray mass spectrometry have been previously used to characterize the kinetics of subunit exchange in multimeric proteins, the magnetic resonance techniques introduced here significantly broaden the array of available tools for characterization of subunit exchange kinetics in protein complexes including protein homodimers, protein heterodimers, protein homo-oligomers, and hetero-oligomeric protein–protein complexes as well as protein-DNA and protein-RNA complexes. While the FRET and mass-spectrometry techniques have an advantage compared to both the PRE- and DEER-based techniques in terms of sensitivity, the magnetic resonance techniques introduced here offer the capability to characterize subunit exchange kinetics under the exact pH, buffer, and concentration conditions used to study the structure and dynamics of protein complexes using complementary magnetic resonance techniques or x-ray crystallization conditions. As a result, these PRE- and DEER-based methods should enable broader investigations of the biological significance of subunit exchange kinetics in protein complexes. Finally, NMR spectroscopists using solution-state NMR methods for structure determination of protein complexes should find practical application of the techniques while preparing samples for ^{13}C-edited/^{12}C-filtered NOESY experiments.

Acknowledgments This work was supported by the National Institute of General Medical Sciences; Protein Structure Initiative-Biology Program; Grant Number U54-GM094597. The majority of the data collection was conducted at the Ohio Center of Excellence in Biomedicine in Structural Biology and Metabonomics at Miami University. We acknowledge Gaetano Montelione, John Everett, and the rest of the Protein Production group at Rutgers University for providing the Dsy0195 mutants used in this study.

References

Aquilina JA, Benesch JLP, Ding LL, Yaron O et al (2005) Subunit exchange of polydisperse proteins. J Biol Chem 280:14485–14491

Battiste JL, Wagner G (2000) Utilization of site-directed spin labeling and high-resolution heteronuclear nuclear magnetic resonance for global fold determination of large proteins with limited nuclear overhauser effect data. Biochemistry 39:5355–5365

Borbat PP, McHaourab HS, Freed JH (2002) Protein structure determination using long-distance constraints from double-quantum coherence ESR: study of T4 lysozyme. J Am Chem Soc 124:5304–5314

Bova MP, Ding L–L, Horwitz J, Fung BK-K (1997) Subunit Exchange of αA-crystallin. J Biol Chem 272:29511–29517

Bova MP, Mchaourab HS, Han Y, Fung BK-K (2000) Subunit exchange of small heat shock proteins. J Biol Chem 275: 1035–1042

Cai SJ, Inouye M (2003) Spontaneous subunit exchange and biochemical evidence for trans-autophosphorylation in a dimer of *E. coli* histidine kinase (EnvZ). J Mol Biol 329:495–503

Clore GM, Tang C, Iwahara J (2007) Elucidating transient macromolecular interactions using paramagnetic relaxation enhancement. Curr Opin Struct Biol 17:603–616

Cooper T, Leifert WR, Glatz RV, McMurchie EJ (2008) Expression and characterisation of functional lanthanide-binding tags fused to a G-protein and muscarinic (M2) receptor. J Bionanosci 2:27–34

Darke PL, Jordan SP, Hall DL, Zugay JA et al (1994) Dissociation and association of the HIV-1 protease dimer subunits: equilibria and rates. Biochemistry 33:98–105

Folmer RH, Hilbers CW, Konings RN, Hallenga K (1995) A (13)C double-filtered NOESY with strongly reduced artefacts and improved sensitivity. J Biomol NMR 5:427–432

Gabdoulline RR, Wade RC (2002) Biomolecular diffusional association. Curr Opinion Struct Biol 12:204–213

Gavin AC, Aloy P, Grandi P, Krause R et al (2006) Proteome survey reveals modularity of the yeast cell machinery. Nature 440: 631–636

Ghimire H, McCarrick RM, Budil DE, Lorigan GA (2009) Significantly improved sensitivity of Q-band PELDOR/DEER experiments relative to X-band is observed in measuring the intercoil

distance of a leucine zipper motif peptide (GCN4-LZ). Biochemistry 48:5782–5784

Goodsell DS, Olsen AJ (2000) Structural symmetry and protein function. Annu Rev Biophys Biomol Struct 29:105–153

Hilger D, Polyhach Y, Padan E, Jung H et al (2007) High-resolution structure of a Na^+/H^+ antiporter dimer obtained by pulsed electron paramagnetic resonance distance measurements. Biophys J 93:3675–3683

Iwahara J, Clore GM (2006) Detecting transient intermediates in macromolecular binding by paramagnetic NMR. Nature 440: 1227–1230

Jeschke G, Abbott RJM, Lea SM, Timmel CR et al (2006a) The characterization of weak protein–protein interactions: evidence from DEER for the trimerization of a von Willebrand factor A domain in solution. Angew Chem Int Ed 45:1058–1061

Jeschke G, Chechik V, Ionita P, Godt A et al (2006b) DeerAnalysis2006—a comprehensive software package for analyzing pulsed ELDOR data. Appl Magn Reson 30:473–498

Lee W, Revington MJ, Arrowsmith C, Kay LE (1994) A pulsed field gradient isotope-filtered 3D ^{13}C HMQC-NOESY experiment for extracting intermolecular NOE contacts in molecular complexes. FEBS Lett 350:87–90

Levy ED, Boeri Erba E, Robinson CV, Teichmann SA (2008) Assembly reflects evolution of protein complexes. Nature 453: 1262–1265

Liang JJ, Liu B-F (2006) Fluorescence resonance energy transfer study of subunit exchange in human lens crystallins and congenital cataract crystallin mutants. Protein Sci 15:1619–1627

Mathhews JM, Sunde M (2012) Dimers, oligomers, everywhere. Adv Exp Med Biol 747:1–18

Nooren IM, Thornton JM (2003) Structural characterisation and functional significance of transient protein–protein interactions. J Mol Biol 325:991–1018

Otting G, Wüthrich K (1989) Extended heteronuclear editing of 2D ^1H NMR spectra of isotope-labeled proteins, using the X(ω1, ω2) double half filter. J Magn Reson 85:586–594

Pannier M, Veit S, Godt A, Jeschke G et al (2000) Dead-time free measurement of dipole–dipole interactions between electron spins. J Magn Reson 142:331–340

Pervushin K, Riek R, Wider G, Wüthrich K (1997) Attenuated T_2 relaxation by mutual cancellation of dipole–dipole coupling and chemical shift anisotropy indicates an avenue to NMR structures of very large biological macromolecules in solution. Proc Natl Acad Sci USA 94:12366–12371

Polyhach Y, Bordignon E, Tschaggelar R, Gandra S et al (2012) High sensitivity and versatility of the DEER experiment on nitroxide radical pairs at Q-band frequencies. Phys Chem Chem Phys 14:10762–10773

Rumpel S, Becker S, Zweckstetter M (2008) High-resolution structure determination of the CylR2 homodimer using paramagnetic relaxation enhancement and structure-based prediction of molecular alignment. J Biomol NMR 40:1–13

Schanda P, Brutscher B (2005) Very fast two-dimensional NMR spectroscopy for real-time investigation of dynamic events in proteins on the time scale of seconds. J Am Chem Soc 127: 8014–8015

Scholosshauer M, Baker D (2004) Realistic protein–protein association rates from a simple diffusional model neglecting long-range interactions, free energy barriers, and landscape ruggedness. Protein Sci 13:1660–1669

Shen HB, Chou KC (2009) Quatldent: a web server for identifying protein quaternary structural attribute by fusing functional domain and sequential evolution information. J Proteome Res 8:1577–1584

Smoluchowski MV (1917) Versuch einer mathematischen theorie der koagulationskinetik kolloider loeschungen. Z Phys Chem 92: 129–168

Sobott F, Benesch JLP, Vierling E, Robinson CV (2002) Subunit exchange of multimeric protein complexes. J Biol Chem 277: 38921–38929

Tang C, Iwahara J, Clore GM (2006) Visualization of transient encounter complexes in protein–protein association. Nature 444: 383–386

Tang C, Schwieters CD, Clore GM (2007) Open-to-closed transition in apo maltose-binding protein observed by paramagnetic NMR. Nature 449:1078–1082

Tang C, Ghirlando R, Clore GM (2008a) Visualization of transient ultra-weak protein self-association in solution using paramagnetic relaxation enhancement. J Am Chem Soc 130:4048–4056

Tang C, Louis JM, Aniana A, Suh JY et al (2008b) Visualizing transient events in amino-terminal autoprocessing of HIV-1 protease. Nature 455:693–696

Uetrecht C, Watts NR, Stahl SJ, Wingfield PT et al (2010) Subunit exchange rates in Hepatitis B virus capsids are geometry- and temperature-dependent. Phys Chem Chem Phys 12:13368–13371

Vinogradova O, Qin J (2012) NMR as a unique tool in assessment and complex determination of weak protein–protein interactions. Top Curr Chem 326:35–45

Ward R, Bowman A, El-Mkami H, Owen-Hughes T et al (2009) Long distance PELDOR measurements on the histone core particle. J Am Chem Soc 131:1348–1349

Yagi H, Banerjee D, Graham B, Huber T, Goldfarb D et al (2011) Gadolinium tagging for high-precision measurements of 6 nm distances in protein assemblies by EPR. J Am Chem Soc 133:10418–10421

Yang Y, Ramelot TA, McCarrick RM, Ni S et al (2010) Combining NMR and EPR methods for homodimer protein structure determination. J Am Chem Soc 132:11910–11913

Yang Y, Ramelot TA, Cort JR, Wang H et al (2011) Solution NMR structure of Dsy0195 homodimer from *Desulfitobacterium hafniense*: first structure representative of the YabP domain family of proteins involved in spore coat assembly. J Struct Funct Genomics 12:175–179

Yu D, Volkov AN, Tang C (2009) Characterizing dynamic protein–protein interactions using differentially scaled paramagnetic relaxation enhancement. J Am Chem Soc 131:17291–17297